Inorg. Chem. **2007**, *46*, 10143–10152

Mononuclear and Polynuclear Copper(I) Complexes with a New N,N′,S-Donor Ligand and with Structural Analogies to the Copper Thionein Core

Marcello Gennari, Maurizio Lanfranchi, Roberto Cammi, Maria Angela Pellinghelli, and Luciano Marchiò*

Dipartimento di Chimica Generale ed Inorganica, Chimica Analitica, Chimica Fisica, Università degli Studi di Parma, v.le G.P. Usberti 17/a, I 43100 Parma, Italy

Received June 18, 2007

The N,N′,S-donor ligand 4-methoxy-3,5-dimethyl-2-((3-(2-(methylthio)phenyl)-1*H*-pyrazol-1-yl)methyl)pyridine (**L**) was prepared from 2-(chloromethyl)-4-methoxy-3,5-dimethylpyridine hydrochloride and 3-(2-(methylthio)phenyl)-1*H*-pyrazole. The Cu(I) complexes $[Cu_2(L)_2CH_3CN][Cu(L)CH_3CN](BF_4)_3$ (**1**), $[Cu(L)PPh_3]BF_4$ (**2**), and $[Cu_6(L)_2(C_6F_5S)_6]$ (**3**) were prepared and characterized by X-ray crystallography (PPh_3 = triphenylphosphine, $C_6F_5S^-$ = pentafluorothiophenolate). The unit cell of compound **1** consists of cocrystallized mononuclear and dinuclear entities in which all of the copper atoms exhibit distorted tetrahedral coordination. Compound **2** is monomeric with **L** bound in the κ^3-N,N′,S mode and a PPh_3 molecule that completes the coordination environment. Compound **2** presents a fluxional behavior in $CDCl_3$ solution due to the boat inversion of the six-membered N,N′ chelate ring ($\Delta H^{\ddagger}$ = +43.6(3) kJ mol^{-1}, $\Delta S^{\ddagger}$ = –16(1) J mol^{-1} K^{-1}). Crystallization of **3** in acetonitrile leads to a polynuclear structure that contains a CH_3CN molecule coordinated to one of the copper atoms: $[Cu_6(L)_2(C_6F_5S)_6CH_3CN]$ (**3a**). The core of **3a** partially resembles a $\{Cu_4S_6\}$ adamantane-like moiety, the only difference being that the Cu–$NCCH_3$ interaction leads to the opening of the cluster by disrupting a Cu–Cu interaction. Part of this assembly is found in the yeast metallothionein copper(I)–cysteinate core whose crystal structure has recently been reported. Two additional $[Cu(L)]^+$ peripheral moieties interact with the cluster by means of bridging thiolates. ESI-mass spectrometry, conductivity measurements, and $^1H/^{19}F$ pulsed gradient spin echo (PGSE) NMR experiments suggest that **3a** dissociates in acetonitrile solution: **3a** + $CH_3CN \rightarrow [Cu_4(C_6F_5S)_6]^{2-} + 2[Cu(L)CH_3CN]^+$. The stability of the cluster with respect to the hypothetical mononuclear species, $[Cu(L)(C_6F_5S)]$, is confirmed by DFT calculations (B3LYP), which illustrate the exergonic character of the reaction: $6[Cu(L')(C_6H_5S)] \rightarrow [Cu_6(L')_2(C_6H_5S)_6] + 4L'$ (ΔG_{298} = –58.6 kJ mol^{-1}, where L′ and $C_6H_5S^-$ are simplified models for **L** and $C_6F_5S^-$, respectively). The energetics pertinent to the ionic dissociation of the cluster in acetonitrile is computed using the polarizable continuum model (PCM) approach.

Introduction

The bioinorganic relevance of copper is evidenced through its involvement in many crucial biological functions.[1] These can be classified as follows: (a) dioxygen activation (tyrosinase[2,3]); (b) dioxygen transport (hemocyanin[4]); (c) electron transfer (blue copper proteins[5−8]); (d) copper delivery, storage, and detoxification (thioneins[9]). The metal coordination is fundamental in the definition of the functional properties of these copper proteins.[10,11]

* To whom correspondence should be addressed. E-mail: marchio@unipr.it.

(1) Malmstrom, B. G.; Leckner, J. *Curr. Opin. Chem. Biol.* **1998**, *2*, 286−292.
(2) Solomon, E. I.; Sundaram, U. M.; Machonkin, T. E. *Chem. Rev.* **1996**, *96*, 2563−2605.
(3) Solomon, E. I.; Chen, P.; Metz, M.; Lee, S. K.; Palmer, A. E. *Angew. Chem., Int. Ed.* **2001**, *40*, 4570−4590.
(4) Solomon, E. I.; Tuczek, F.; Root, D. E.; Brown, C. A. *Chem. Rev.* **1994**, *94*, 827−856.
(5) Colman, P. M.; Freeman, H. C.; Guss, J. M.; Murata, M.; Norris, V. A.; Ramshaw, J. A. M.; Venkatappa, M. P. *Nature* **1978**, *272*, 319−324.
(6) Durley, R.; Chen, L. Y.; Mathews, F. S.; Davidson, V. L. *Protein Sci.* **1993**, *2*, 739−752.
(7) Hart, P. J.; Nersissian, A. M.; Herrmann, R. G.; Nalbandyan, R. M.; Valentine, J. S.; Eisenberg, D. *Protein Sci.* **1996**, *5*, 2175−2183.
(8) Shibata, N.; Inoue, T.; Nagano, C.; Nishio, N.; Kohzuma, T.; Onodera, K.; Yoshizaki, F.; Sugimura, Y.; Kai, Y. *J. Biol. Chem.* **1999**, *274*, 4225−4230.

10.1021/ic701189b CCC: $37.00
Published on Web 11/01/2007

Scheme 1

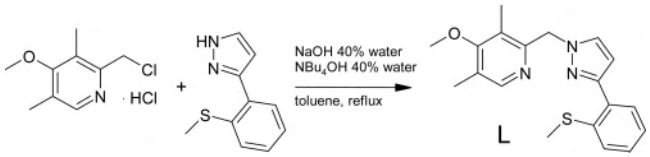

We are interested in preparing new Cu complexes with nitrogen−sulfur donor ligands suitable as mimics of copper sites in biological systems. Previously, we employed scorpionate boron-centered ligands to reproduce the metal coordination environment of blue copper proteins in their reduced state, but their stereochemical flexibility and low tunability in terms of donor atom types posed considerable limits for the role of their respective Cu complexes as good functional models.[12] For this reason, we directed our interest toward new ligand structures that may be able to bind copper in a ligand-determined geometric environment. The facile synthesis of a variously substituted pyrazole−pyridine platform[13] prompted us to investigate the coordination ability of new ligands belonging to this class with opportune pyrazole substituents (Scheme 1). It is noteworthy that, due to the easy deprotonation of the bridging methylene group and further functionalization, these ligands can be considered as parent compounds for the synthesis of new scorpionates, which should produce a more preorganized coordination environment.

In this work, we used a thioether-substituted pyrazole, 3-(2-(methylthio)phenyl)pyrazole, which is known to bind Cu(II) once incorporated in a N_3S_3 hydrotris(pyrazolyl)borato derivative,[14] as a precursor. Here we describe the coordination properties of the new N,N′,S-donor ligand **L** with copper(I). To complete the coordination at the metal, PPh_3 and $C_6F_5S^-$ were also employed as coligands. The crystal structures of $[Cu_2(L)_2CH_3CN][Cu(L)CH_3CN](BF_4)_3$ (**1**), $[Cu(L)PPh_3]BF_4$ (**2**), and $[Cu_6(L)_2(C_6F_5S)_6CH_3CN]$ (**3a**) are reported, and they point to a certain coordination flexibility of **L**, which appears not to be able to impose a definite geometry at the metal. After using PPh_3, which led to the isolation of **2** as a mononuclear complex, we employed the $C_6F_5S^-$ thiolate ligand to mimic the $^-$S-Cys fragment of proteins. In the present case, the ternary ensemble Cu(I)/**L**/$C_6F_5S^-$ affords the polynuclear structure **3**, which can be rationalized in terms of the general property of the thiolates to form M−S−M bridges[15−18] and by the lack of specific steric hindrance on the ligand **L**. This copper−sulfur structural arrangement can be found in metallothionein models,[19] and it bears similarities with the copper(I)−thiolate core of the yeast copper thionein, whose crystal structure has recently been reported.[20] We also wished to evaluate the stability of the cluster structure of **3** in solution. For this purpose, ^{1}H and ^{19}F PGSE (pulsed gradient spin echo) NMR spectroscopy was employed,[21] affording a hydrodynamic radius (r_H) and the corresponding volume (V_H), which are consistent with the multinuclear solid-state structure, even though some degree of dissociation of **3** into the $[Cu_4(C_6F_5S)_6]^{2-}$ and $[Cu(L)CH_3CN]^+$ ions can be envisaged. This hypothesis was also supported by conductivity measurements and ESI-mass spectrometry. DFT calculations were also employed to investigate the stability of **3** with respect to the hypothetical mononuclear entity $[Cu(L)(C_6F_5S)]$ and to investigate the stability of the $[Cu_4(C_6F_5S)_6]^{2-}$ moiety in the presence of a coordinating solvent such as acetonitrile. The PCM (polarizable continuum model)[22] approach was employed to evaluate the influence of the solvent on the ionic dissociation energy of the cluster.

Experimental Methods

General Procedures. All reagents and solvents were commercially available, except for 3-(2-(methylthio)phenyl)-1*H*-pyrazole[14] and $[Cu(CH_3CN)_4]BF_4$,[23] which were prepared as previously reported. Dichloromethane and acetonitrile were dried over CaH_2 and distilled before use. The syntheses of the complexes were performed in inert gas (N_2) using Schlenk techniques.

Synthesis of 4-Methoxy-3,5-dimethyl-2-((3-(2-(methylthio)-phenyl)-1*H*-pyrazol-1-yl)methyl)pyridine (L). 2-(Chloromethyl)-4-methoxy-3,5-dimethylpyridine hydrochloride (5.84 g, 26.29 mmol) and 3-(2-(methylthio)phenyl)-1*H*-pyrazole (5.00 g, 26.28 mmol) were mixed in toluene (150 mL). After addition of a 40% NaOH water solution (50 mL) and a 40% NBu_4OH water solution (30 drops), the mixture was refluxed for 3 h. The organic phase was separated, washed with water (30 mL), and dried with Na_2SO_4. The solvents were removed under vacuum. Purification of the product by flash chromatography using ethyl acetate as the eluent produced a yellow oil, which was washed and triturated with hexane and finally dried under vacuum, yielding a light orange microcrystalline powder (5.35 g, 15.77 mmol, 60%). Colorless crystals suitable for X-ray diffraction were obtained by layering hexane over a dichloromethane solution of the product, corresponding to **L**. IR (cm^{-1}): 3146 w, 3122 m, 3059 w, 3047 w, 2999 m, 2957 m, 2943 m, 2918 m, 1586 m, 1569 m, 1480 m, 1450 s, 1437 m, 1401 m, 1332 m, 1255s, 1213 m, 1086 m, 1050 m, 999 m, 867 w br, 753 vs. ^{1}H NMR (300 MHz, $CDCl_3$): δ 2.28 (s, 3H, CH_3 py *o*-CH), 2.33 (s, 3H, CH_3 py *p*-CH), 2.43 (s, 3H, CH_3S), 3.77 (s, 3H, CH_3O), 5.51 (s, 2H, CH_2), 6.60 (d, J = 2.2 Hz, 1H, CH pz(ph)), 7.18 (dt, J = 7.0, 1.9 Hz, 1H, CH ph), 7.29 (m, 2H, CH ph), 7.45 (d, J =

(9) Chan, J. N.; Huang, Z. Y.; Merrifield, M. E.; Salgado, M. T.; Stillman, M. J. *Coord. Chem. Rev.* **2002**, *233*, 319−339.
(10) Belle, C.; Rammal, W.; Pierre, J. L. *J. Inorg. Biochem.* **2005**, *99*, 1929−1936.
(11) Holm, R. H.; Kennepohl, P.; Solomon, E. I. *Chem. Rev.* **1996**, *96*, 2239−2314.
(12) Cammi, R.; Gennari, M.; Giannetto, M.; Lanfranchi, M.; Marchio, L.; Mori, G.; Paiola, C.; Pellinghelli, M. A. *Inorg. Chem.* **2005**, *44*, 4333−4345.
(13) Gennari, M.; Tegoni, M.; Lanfranchi, M.; Pellinghelli, M. A.; Marchio, L. *Inorg. Chem.* **2007**, *46*, 3367−3377.
(14) Humphrey, E. R.; Mann, K. L. V.; Reeves, Z. R.; Behrendt, A.; Jeffery, J. C.; Maher, J. P.; McCleverty, J. A.; Ward, M. D. *New J. Chem.* **1999**, *23*, 417−423.
(15) Dance, I. G. *Polyhedron* **1986**, *5*, 1037−1104.
(16) Fujisawa, K.; Imai, S.; Kitajima, N.; Moro-oka, Y. *Inorg. Chem.* **1998**, *37*, 168−169.
(17) Henkel, G.; Krebs, B. *Chem. Rev.* **2004**, *104*, 801−824.
(18) Coucouvanis, D.; Murphy, C. N.; Kanodia, S. K. *Inorg. Chem.* **1980**, *19*, 2993−2998.
(19) Presta, A.; Fowle, D. A.; Stillman, M. J. *J. Chem. Soc., Dalton Trans.* **1997**, 977−984.
(20) Calderone, V.; Dolderer, B.; Hartmann, H. J.; Echner, H.; Luchinat, C.; Del, Bianco, C.; Mangani, S.; Weser, U. *Proc. Natl. Acad. Sci. U.S.A.* **2005**, *102*, 51−56.
(21) Zuccaccia, D.; Macchioni, A. *Organometallics* **2005**, *24*, 3476−3486.
(22) Tomasi, J.; Mennucci, B.; Cammi, R. *Chem. Rev.* **2005**, *105*, 2999−3093.
(23) Leftin, J. H. *Chem. Abstr*. **1967**, *66*, 46487e.

2.2 Hz, 1H, CH pz(CH_2)), 7.56 (d, J = 7.4 Hz, 1H, CH ph), 8.26 (s, 1H, CH py). ^{13}C NMR (75 MHz, $CDCl_3$): 10.7 (CH_3 py *p*-CH), 13.0 (CH_3 py *o*-CH), 15.7 (CH_3S), 56.1 (CH_2), 59.5 (CH_3O), 106.2 (CH pz(ph)), 124.1 (CH ph), 124.9 (CH ph), 125.9 (C quat py), 125.9 (C quat py), 127.7 (CH ph), 129.2 (CH pz(CH_2R)), 129.3 (CH ph), 132.1 (C quat ph), 137.0 (C quat ph), 149.0 (CH py), 149.6 (C quat), 153.4 (C quat), 164.0 (C quat CH_3O). ESI-MS (p.i., cone 50 V, MeOH, *m*/*z*, *I* %): 340.5, 100, $[LH]^+$. Anal. Calcd for $C_{19}H_{21}N_3OS$ (M_r = 339.46): C, 67.23; H, 6.23; N, 12.38. Found: C, 67.14; H, 6.30; N, 12.44.

Synthesis of $[Cu_2(L)_2CH_3CN][Cu(L)CH_3CN](BF_4)_3$ (1). A solution of $[Cu(CH_3CN)_4]BF_4$ (264 mg, 0.84 mmol) in dichloromethane (20 mL) was added to a solution of **L** (272 mg, 0.80 mmol) in dichloromethane (20 mL) at room temperature while stirring. After 1 h, the solution was concentrated to ~5 mL under vacuum; a white product was precipitated with hexane (25 mL) and then filtered out and dried under vacuum, yielding a colorless powder (**1**, 250 mg, 0.16 mmol, 62%). Colorless crystals suitable for X-ray diffraction were obtained by evaporation from an acetonitrile−water solution of the product. IR (cm^{-1}): 3138 m, 3016 w, 2946 w, 1591 m, 1521 w, 1494 m, 1473 s, 1434 s, 1411 m, 1366 m, 1298 m, 1256 s, ~1050 vs br, 761 s. ^{1}H NMR (300 MHz, CD_2Cl_2): δ 2.22 (s br, 6H, CH_3 py), 2.48 (s, 3H, CH_3S), 3.82 (s br, 3H, CH_3O), 5.29 (s br, 2H, CH_2), 6.43 (s br, 1H, CH pz(ph)), 7.45 (s br, 4H, CH(ph)), 7.87 (s br, 1H, CH pz(CH_2), 8.20 (s br, 1H, CH py). ^{13}C NMR (75 MHz, CD_2Cl_2): δ 2.80, 11.40, 13.29, 20.89, 51.90, 60.41, 106.40, 127.55, 128.28, 129.37, 129.70, 130.28, 131.02, 131.75, 132.16, 132.60, 148.85, 151.08, 165.64. Anal. Calcd for $C_{61}H_{69}B_3F_{12}N_{11}O_3S_3Cu_3$ (M_r = 1551.54): C, 47.22; H, 4.48; N, 9.93. Found: C, 47.02; H, 4.35; N, 9.49.

Synthesis of $[Cu(L)PPh_3]BF_4$ (2). A solution of $[Cu(CH_3CN)_4]BF_4$ (195 mg, 0.62 mmol) in acetonitrile (5 mL) was added to a solution of **L** (206 mg, 0.61 mmol) and PPh_3 (155 mg, 0.59 mmol) in acetonitrile (20 mL) at room temperature while stirring. After 1 h, the solution was dried under a vacuum, producing a colorless solid, which was recrystallized in dichloromethane−hexane, yielding a white powder (**2**, 400 mg, 0.53 mmol, 90%). Colorless crystals suitable for X-ray diffraction were obtained by layering hexane over a THF solution of the product. IR (cm^{-1}): 3139 w, 3054 w, 3005 w, 1591 m, 1569 m, 1475 m, 1433 s, 1256 m, 1061 vs br, 755 s br, 695 s. ^{1}H NMR (300 MHz, $CDCl_3$): δ 1.78 (s, 3H, CH_3S), 2.20 (s, 3H, CH_3 py *o*-CH), 2.57 (s, 3H, CH_3 py *p*-CH), 3.82 (s, 3H, CH_3O), 5.49 (s br, 2H, CH_2), 6.52 (s, 1H, CH pz(ph)), 7.15−7.30 (m, 17H, CH ph), 7.46 (t, J = 6.9 Hz, 1H, CH ph), 7.58 (d, J = 7.2 Hz, 1H, CH ph), 7.99 (s, 1H, CH py), 8.25 (s, 1H, CH pz(CH_2)). ESI-MS (p.i., cone 29 V, MeOH, *m*/*z*, *I* %): 402.2, 100, $[Cu(L)]^+$; 664.2, 70, $[Cu(L)PPh_3]^+$. Anal. Calcd for $C_{37}H_{36}BF_4N_3OPSCu$ (M_r = 752.09): C, 59.09; H, 4.82; N, 5.59. Found: C, 59.17; H, 4.90; N, 5.51.

Synthesis of $[Cu_6(L)_2(C_6F_5S)_6]$ (3). L (720 mg, 2.12 mmol) was added to a suspension of CuCl (630 mg, 6.36 mmol) in acetonitrile (20 mL), which then produced an orange solution. After few minutes, C_6F_5SH (0.85 mL, d = 1.5 g/mL, 6.37 mmol) and NH_4OH 15.71 M (0.41 mL, 6.44 mmol) were added, with consequent formation of a precipitate. After 30 min, water (10 mL) was added and the white solid was filtered out and dried under vacuum, yielding a bright yellow powder (**3**, 1.68 g, 0.74 mmol, 70%). IR (cm^{-1}): ~2920 w, 1636 w, 1626 w, 1508 vs, 1473 vs, 1373 w, 1357 w, 1294 w, 1260 w, 1138 w, 1082 vs, 1009 w, 968 vs, 850 vs, 761 w. Anal. Calcd for $C_{74}H_{42}F_{30}N_6O_2S_8Cu_6$ (M_r = 2254.92): C, 39.42; H, 1.88; N, 3.73. Found: C, 39.51; H, 1.79; N, 3.65. Colorless crystals suitable for X-ray diffraction were obtained by cooling to 8 °C an acetonitrile−water solution of **3**, corresponding to $[Cu_6(L)_2(C_6F_5S)_6CH_3CN]$ (**3a**). The solution characterization of **3** was performed in acetonitrile (see Results and Discussion). ^{1}H NMR (300 MHz, CD_3CN): δ 2.12 (s, 3H, CH_3), 2.20 (s, 3H, CH_3), 2.42 (s, 3H, CH_3S), 3.78 (s, 3H, CH_3O), 5.50 (s, 2H, CH_2), 6.50 (d, J = 2.2 Hz, 1H, CH pz(ph)), 7.30 (m, 3H, CH ph), 7.42 (m, 1H, CH ph), 7.83 (d, J = 2.2 Hz, 1H, CH pz(CH_2)), 8.16 (s, 1H, CH py). ^{13}C NMR (75 MHz, CD_3CN): δ 11.7, 13.4, 18.2, 53.0, 107.0, 128.0, 129.8, 130.1, 131.3, 132.8, 136.3 (m), 139.6 (m), 145.4 (m), 148.5 (m), 151.3. ^{19}F NMR (564 MHz, CD_3CN): δ −200.7 (d, J = 28 Hz, 2F), −233.0 (t, J = 25 Hz, 1F), −233.8 (t, J = 23 Hz, 2F). ESI-MS (n.i., cone −41 V, CH_3CN, *m*/*z*, *I* %): 461.0, 100, $[Cu(C_6F_5S)_2)]^-$; 724.8, 25, $[Cu_2(C_6F_5S)_3)]^-$; 986.6, 30, $[Cu_3(C_6F_5S)_4)]^-$; 1248.7, 12, $[Cu_4(C_6F_5S)_5)]^-$; 1512.5, 8, $[Cu_5(C_6F_5S)_6)]^-$. ESI-MS (p.i., cone 85 V, CH_3CN, *m*/*z*, *I* %): 387.3, 100; 402.3, 40, $[Cu(L)]^+$.

Physical Techniques. ^{1}H, ^{13}C, and 2D NMR spectra were recorded on a Bruker Avance 300 spectrometer using standard Bruker pulse sequences. Chemical shifts are reported in ppm referenced to residual solvent protons ($CDCl_3$, CD_2Cl_2, CD_3CN). ^{1}H and ^{19}F PGSE NMR measurements were performed in a solution of **3** (10^{-3} M) in CD_3CN using a standard stimulated echo (STE) sequence on a Varian Inova spectrometer (600 MHz) at 300 K and without spinning. An external reference (trifluorotoluene, −63.72 ppm) was used for the ^{19}F chemical shift calibration. Tetrakis(methylsilyl)silane (TMSS, hydrodynamic radius $r_H \approx r_{vdw}$ = 4.28 Å) was used as an internal standard. The hydrodynamic radius (r_H) and volume ($V_H = (4/3)\pi r_H^3$) were obtained as described in the literature (Supporting Information).[21,24] The van der Waals volumes (V_{vdW}) and the solvent-excluded volumes (V_{soft})[25] were computed on **3a** and on the mononuclear unit of **1** starting from the X-ray coordinates using the software package DS Viewer Pro 5.0.

Mass spectra were obtained with a Micromass ZMD spectrometer. The mixtures were analyzed in the positive and negative ionization modes by direct perfusion in ESI-MS interface. Infrared spectra were recorded from 4000 to 700 cm^{-1} on a Perkin-Elmer FT-IR Nexus spectrometer equipped with a Thermo-Nicolet microscope. Elemental analyses (C, H, N) were performed with a Carlo Erba EA 1108 automated analyzer. The luminescence spectrum of **3** (yellow powder) was recorded on a Horiba Jobin Yvon SPEX FluoroMax 4 spectrofluorometer, using a UG11 band-pass filter on the excitation slit and a long-pass filter GG475 on the emission slit. Conductivity measurements were performed on a Crison microCM 2202 conductometer operating at 25 °C.

X-ray Crystallography. A summary of data collection and structure refinement for **L**, **1**, **2**, and **3a** is reported in Table 1. Single-crystal data were collected with a Bruker Smart 1000 area detector diffractometer (Mo Kα; λ = 0.710 73 Å). Cell parameters were refined from the observed setting angles and detector positions of selected strong reflections. Intensities were integrated from several series of exposure frames covering the sphere of reciprocal space.[26] No crystal decay was observed. Absorption corrections using the program SADABS[27] was applied for **L**, **2**, and **3a**, which resulted in transmission factors ranging from 0.720 to 1.000 (**L**), 0.653 to 1.000 (**2**), and 0.834 to 1.000 (**3a**), whereas the program

(24) Pregosin, P. S. *Prog. Nucl. Magn. Reson. Spectrosc.* **2006**, *49*, 261−288.
(25) V_{soft} is calculated by considering that the interstitial parts of the solute molecule are not accessible to the solvent. The solvent-excluded volume is the sum of the Van der Waals volume plus the interstitial volume. See: Connolly, M. L. *J. Am. Chem. Soc.* **1985**, *107*, 1118−1124.
(26) *SMART (control) and SAINT (integration) software for CCD systems*; Bruker AXS, Madison, WI, 1994.
(27) *Area-Detector Absorption Correction*; Siemens Industrial Automation Inc.: Madison, WI, 1996.

Table 1. Summary of X-ray Crystallographic Data for **L**, **1**, **2**, and **3a**

param	L	1	2	3a
empirical formula	$C_{38}H_{42}N_2S_2$	$C_{61}H_{69}B_3Cu_3F_{12}N_{11}O_3S_3$	$C_{37}H_{36}B_4CuF_4N_3OPS$	$C_{76}H_{45}Cu_6F_{30}N_7O_2S_8$
fw	678.90	1551.50	752.07	2295.91
color, habit	colorless, block	colorless, block	colorless, block	colorless, plate
cryst size, mm	0.45 × 0.20 × 0.15	0.18 × 0.10 × 0.08	0.38 × 0.30 × 0.10	0.35 × 0.15 × 0.10
cryst system	monoclinic	monoclinic	triclinic	triclinic
space group	$P2_1/c$	$P2_1$	$P\bar{1}$	$P\bar{1}$
a, Å	16.984(3)	12.430(9)	10.431(1)	15.502(2)
b, Å	7.628(1)	20.105(9)	12.378(1)	16.672(2)
c, Å	28.302(5)	14.665(8)	15.213(2)	18.535(2)
α, deg	90	90	78.13(1)	106.93(1)
β, deg	98.15(1)	107.10(3)	78.95(1)	100.92(1)
γ, deg	90	90	70.41(1)	93.45(1)
V, Å^3	3630(1)	3503(4)	1794.8(3)	4465.7(9)
Z	4	2	2	2
T, K	293(2)	293(2)	293(2)	293(2)
ρ(calcd), Mg/m^3	1.242	1.471	1.392	1.707
μ, mm^{-1}	0.188	1.075	1.766	1.701
θ range, deg	1.45−27.04	1.45−24.00	1.77−27.97	1.35−25.00
no. of rflcns/obsvns	38 065/4095	10 942/4747	19 539/4898	42 725/3759
GooF	1.006	0.892	1.009	0.979
Flack param		0.04(1)		
R1[a]	0.0409	0.0587	0.0357	0.0780
wR2[a]	0.0841	0.0675	0.0683	0.0843

[a] $R1 = \sum||F_o| - |F_c||/\sum|F_o|$; $wR2 = [\sum[w(F_o^2 - F_c^2)^2]/\sum[w(F_o^2)^2]]^{1/2}$, $w = 1/[\sigma^2(F_o^2) + (aP)^2 + bP]$, where $P = [\max(F_o^2,0) + 2F_c^2]/3$.

XABS2[28] was used for **1** (maximum and minimum absorption correction coefficients of 1.000−0.497). For **1**, the space group ($P2_1$) was chosen on the basis of the systematic extinction and intensity statistics; the absolute configuration has been confirmed at the 3σ level of the Flack parameter (0.04(1)).[29] The structures were solved by direct methods (SIR97)[30] and refined with full-matrix least squares (SHELXL-97),[31] using the Wingx software package.[32] Non-hydrogen atoms were refined anisotropically for **L** and **2**. The BF_4^- anions in **1** were severely disordered and were refined isotropically. The carbon atoms in **3a** were also refined isotropically due to the poor quality of the crystal and the limited number of observed reflections available. The hydrogen atoms were placed at their calculated positions. Ortep diagrams were prepared using the ORTEP-3 for Windows program.[33]

DFT Calculations. Theoretical calculations were carried out using the Gaussian 03 program suite.[34] Geometry optimization of the mononuclear model compound [Cu(L′)(C_6H_5S)] was performed starting from a pseudotetrahedral copper coordination as found in **2**, by substituting PPh_3 with $C_6H_5S^-$ and by substituting the $-CH_3$ and $-OCH_3$ groups of the pyridine ring of **L** with hydrogen atoms, thus giving the model ligand L′. The CH_3CN molecule and the isolated model ligand L′ were also optimized. The complex [Cu(L′)CH_3CN]$^+$ was optimized by starting from the X-ray coordinates of the mononuclear species of **1**. The polynuclear model complexes [Cu_6(L′)$_2$(C_6H_5S)$_6$] and [Cu_4(C_6H_5S)$_6$]$^{2-}$ were optimized by starting from the [Cu_4(C_6F_5S)$_6$]$^{2-}$ adamantane-like core as found in various copper(I)−thiolate clusters,[17] whereas [Cu_4(C_6H_5S)$_6$$CH_3CN$]$^{2-}$ was optimized starting from the X-ray geometry of **3a** by removing the peripheral [Cu(L)]$^+$ moieties. The gradient-corrected hybrid density functional B3LYP[35,36] and the lanl2dz basis set with Hay and Wadt effective core potential (ECP) were employed.[37,38] Vibrational frequencies were calculated at the same level of theory to ensure that the stationary points were true minima and for the calculation of zero-point energies. Thermal corrections and free energy of reaction were calculated at 298 K. In order to take into account the effect of the solvent on the energy of reactions involving ionic dissociation, the solvation energies (ΔG^{solv}) were estimated using the polarizable continuum model (PCM)[39−42] at the B3LYP/lanl2dz level. ΔG^{solv} represents the energy required to bring a molecule of solute from the gas phase to a polarizable dielectric media. This requires the opening of a cavity in the solvent where the solute can be fitted (ΔG^{cav}), giving rise to solvent−solute electrostatic interactions (ΔG^{eletr}), to van der Waals solvent−solute contributions (ΔG^{disp}), and to some steric repulsion (ΔG^{rep}), so that $\Delta G^{solv} = \Delta G^{cav} + \Delta G^{rep} + \Delta G^{disp} + \Delta G^{electr}$.[43] Single-point energy calcula-

(28) Parkin, S.; Moezzi, B.; Hope, H. *J. Appl. Crystallogr.* **1995**, *28*, 53−56.
(29) Flack, H. D. *Acta Crystallogr.* **1983**, *A39*, 876−881.
(30) Altomare, A.; Burla, M. C.; Camalli, M.; Cascarano, G. L.; Giacovazzo, C.; Guagliardi, A.; Moliterni, A. G. G.; Polidori, G.; Spagna, R. *J. Appl. Crystallogr.* **1999**, *32*, 115−119.
(31) Sheldrick, G. M. *SHELX97. Programs for Crystal Structure Analysis*, release 97-2; University of Göttingen: Göttingen, Germany, 1997.
(32) Farrugia, L. J. *J. Appl. Crystallogr.* **1999**, *32*, 837−838.
(33) Farrugia, L. J. *J. Appl. Crystallogr.* **1997**, *30*, 568.
(34) Frisch, M. J.; Trucks, G. W.; Schlegel, H. B.; Scuseria, G. E.; Robb, M. A.; Cheeseman, J. R.; Montgomery, J. A., Jr.; Vreven, T.; Kudin, K. N.; Burant, J. C.; Millam, J. M.; Iyengar, S. S.; Tomasi, J.; Barone, V.; Mennucci, B.; Cossi, M.; Scalmani, G.; Rega, N.; Petersson, G. A.; Nakatsuji, H.; Hada, M.; Ehara, M.; Toyota, K.; Fukuda, R.; Hasegawa, J.; Ishida, M.; Nakajima, T.; Honda, Y.; Kitao, O.; Nakai, H.; Klene, M.; Li, X.; Knox, J. E.; Hratchian, H. P.; Cross, J. B.; Bakken, V.; Adamo, C.; Jaramillo, J.; Gomperts, R.; Stratmann, R. E.; Yazyev, O.; Austin, A. J.; Cammi, R.; Pomelli, C.; Ochterski, J. W.; Ayala, P. Y.; Morokuma, K.; Voth, G. A.; Salvador, P.; Dannenberg, J. J.; Zakrzewski, V. G.; Dapprich, S.; Daniels, A. D.; Strain, M. C.; Farkas, O.; Malick, D. K.; Rabuck, A. D.; Raghavachari, K.; Foresman, J. B.; Ortiz, J. V.; Cui, Q.; Baboul, A. G.; Clifford, S.; Cioslowski, J.; Stefanov, B. B.; Liu, G.; Liashenko, A.; Piskorz, P.; Komaromi, I.; Martin, R. L.; Fox, D. J.; Keith, T.; Al-Laham, M. A.; Peng, C. Y.; Nanayakkara, A.; Challacombe, M.; Gill, P. M. W.; Johnson, B.; Chen, W.; Wong, M. W.; Gonzalez, C.; Pople, J. A. *Gaussian 03*, revision C.02; Gaussian, Inc.: Wallingford, CT, 2004.
(35) Becke, A. D. *Phys. Rev. A: At., Mol., Opt. Phy.* **1988**, *38*, 3098−3100.
(36) Becke, A. D. *J. Chem. Phys.* **1993**, *98*, 5648−5652.
(37) Hay, P. J.; Wadt, W. R. *J. Chem. Phys.* **1985**, *82*, 299−310.
(38) Wadt, W. R.; Hay, P. J. *J. Chem. Phys.* **1985**, *82*, 284−298.
(39) Tomasi, J.; Mennucci, B.; Cances, E. *J. Mol. Struct.* **1999**, *464*, 211−226.
(40) Mennucci, B.; Cances, E.; Tomasi, J. *J. Phys. Chem. B* **1997**, *101*, 10506−10517.
(41) Mennucci, B.; Tomasi, J. *J. Chem. Phys.* **1997**, *106*, 5151−5158.
(42) Cances, E.; Mennucci, B.; Tomasi, J. *J. Chem. Phys.* **1997**, *107*, 3032−3041.
(43) Cossi, M.; Barone, V.; Cammi, R.; Tomasi, J. *Chem. Phys. Lett.* **1996**, *255*, 327−335.

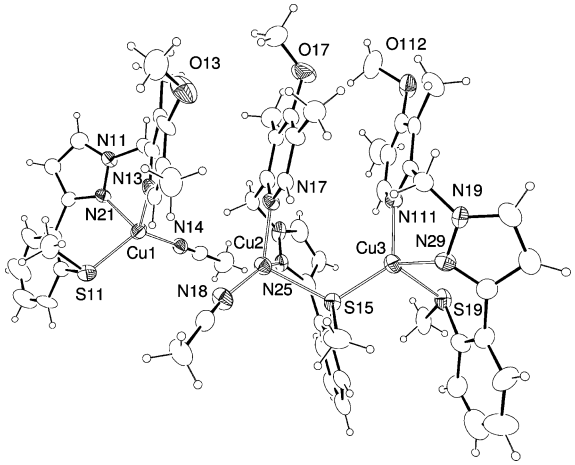

Figure 1. Ortep drawing of **1** at the 30% thermal ellipsoids probability level. A mononuclear and a dinuclear unit are present in the unit cell.

Scheme 2. Thermodynamic Cycle for the Calculation of the Reactions Free Energies in Solution, $\Delta G^{solution} = \Delta G_{298} + \Delta\Delta G^{solv}$ ($\Delta\Delta G^{solv} = \Delta G_P{}^{solv} - \Delta G_R{}^{solv}$)

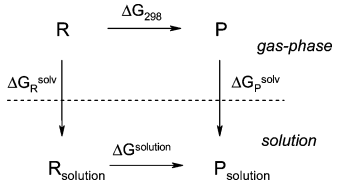

tions at the PCM level were performed on the gas-phase structures without further optimization, assuming that the stationary points in the gas phase are also stationary points in solution. We therefore approximated ΔG^{solv} as the difference between the free energy in solution (G^{solv}) and the gas-phase total energy (E) without zero-point or thermal correction. Inside the cavity that hosts the solute, the dielectric constant is the same as in vacuum, whereas outside it takes the value of the solvent (acetonitrile, $\epsilon = 36.6$). Finally, the free energy of reaction in solution ($\Delta G^{solution}$) was computed as the sum of the gas-phase free energy (ΔG_{298}) and the solvation free energy $\Delta G^{solution} = \Delta G_{298} + \Delta\Delta G^{solv}$ (where $\Delta\Delta G^{solv} = \Delta G_P{}^{solv} - \Delta G_R{}^{solv}$), according to the thermodynamic cycle reported in Scheme 2.

Results and Discussion

Solid-State Structure of $[Cu_2(L)_2CH_3CN][Cu(L)CH_3CN](BF_4)_3$ (1). At first, the coordination capabilities of the N,N′,S-donor ligand **L** versus Cu(I) were tested through reaction with $[Cu(CH_3CN)_4]BF_4$ in acetonitrile in a 1:1 ratio to yield compound **1**. As can be seen in Figure 1, a mononuclear and a dinuclear complex cocrystallize in the unit cell. The first entity is comprised of a copper(I) center, Cu(1), bound by a κ^3-N,N′,S chelate ligand and a CH_3CN molecule. The metal geometry is distorted tetrahedral since the coordination angles range from 122.1(3) to 89.6(3)°. The dinuclear unit exhibits two metal centers in different coordination environments. In particular, Cu(2) is bound by an acetonitrile molecule and by a N,N′S chelate ligand, which in turn bridges to the Cu(3) atom with the thioether sulfur atom S(15). The coordination of Cu(3) is completed by another N,N′S chelate ligand. Interestingly, the bond distances (Table 2) within the sulfur bridge are not equivalent since Cu(3)−S(15) (2.230(3) Å) is significantly shorter than Cu(2)−S(15) (2.462(3) Å). This is related to the different geometry of the Cu(2) and Cu(3) atoms since the latter exhibits a more regular tetrahedral geometry, which is distorted as a consequence of the constraints imposed by the chelate ligand. Conversely, Cu(2) is in a tetrahedral geometry severely distorted toward the trigonal one (equatorial atoms: N(17), N(25), N(18)) due to the long Cu(2)−S(15) interaction. The nearly trigonal geometry of Cu(2) is supported by the sum of the equatorial angle values, 353.1(3)°, which is close to the theoretical value of 360°, and by the fact that Cu(2) is only 0.282(1) Å out of the equatorial plane and is directed toward the apical sulfur S(15). The three metals are stereogenic centers, and they all exhibit an *S* configuration. Interestingly, this leads to a spontaneous resolution at the solid state since **1** crystallizes in the chiral space group $P2_1$. Each of the three BF_4^- counterions are disordered in two positions that roughly define a spherical structural site occupation. In light of these results, it can be concluded that the nuclearity of **1** cannot be defined a priori, due to the flexibility and the lack of appropriate sterical hindrance of **L**.

Table 2. Selected Bond Lengths (Å) for **1**, **2**, and **3a**

	Compound **1**		
Cu(1)−S(11)	2.304(3)	Cu(2)−N(17)	2.044(7)
Cu(1)−N(21)	2.033(7)	Cu(2)−N(18)	1.890(8)
Cu(1)−N(13)	2.054(8)	Cu(3)−S(15)	2.230(3)
Cu(1)−N(14)	1.919(9)	Cu(3)−S(19)	2.390(3)
Cu(2)−S(15)	2.462(3)	Cu(3)−N(29)	2.016(6)
Cu(2)−N(25)	1.988(7)	Cu(3)−N(111)	2.062(7)
	Compound **2**		
Cu−S(11)	2.4482(7)	Cu−N(13)	2.092(2)
Cu−P(14)	2.1957(7)	Cu−N(21)	2.014(2)
	Compound **3a**		
Cu(1)−N(21)	1.937(8)	Cu(4)−S(19)	2.214(3)
Cu(1)−N(13)	2.072(7)	Cu(5)−S(18)	2.234(4)
Cu(1)−S(17)	2.156(3)	Cu(5)−S(19)	2.259(3)
Cu(2)−N(16)	2.028(8)	Cu(5)−N(1)	1.88(1)
Cu(2)−N(24)	2.03(1)	Cu(6)−S(17)	2.297(3)
Cu(2)−S(14)	2.399(4)	Cu(6)−S(18)	2.341(3)
Cu(2)−S(111)	2.254(3)	Cu(6)−S(112)	2.244(3)
Cu(3)−S(110)	2.261(3)	Cu(4)−Cu(5)	2.768(2)
Cu(3)−S(111)	2.223(3)	Cu(5)−Cu(6)	2.814(2)
Cu(3)−S(112)	2.244(3)	Cu(4)−Cu(6)	2.842(2)
Cu(4)−S(110)	2.241(3)	Cu(3)−Cu(4)	3.489(2)
Cu(4)−S(17)	2.330(3)	Cu(3)−Cu(6)	3.396(2)

Solid-State Structure and Solution Properties of $[Cu(L)PPh_3]BF_4$ (2). The hypothesis that an ancillary σ-donor ligand such as PPh_3 would complement the coordination properties of **L** to yield a mononuclear species has led to the synthesis and isolation of **2**. The copper coordination is achieved through the N(21), N(13), and S(11) atoms of **L** and by PPh_3, Figure 2. The metal geometry is intermediate between trigonal pyramidal and tetrahedral: the trigonal plane can be defined by P(14), N(21), and N(13) with S(11) in the apical position (Cu−S(11) = 2.4482(7) Å). This geometry is supported by the following criteria: (i) The sum of equatorial angles is 344.23(5)° (cf. 328.5° for a tetrahedral geometry and 360° for trigonal planar geometry). (ii) The

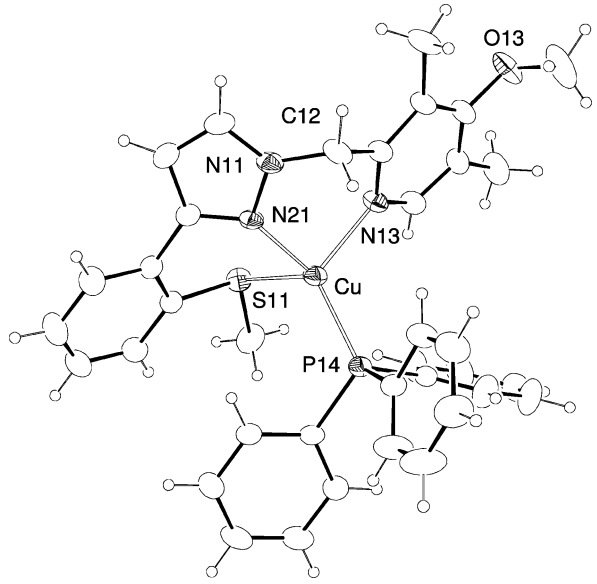

Figure 2. Ortep drawing of the cationic unit of **2** at the 30% thermal ellipsoids probability level.

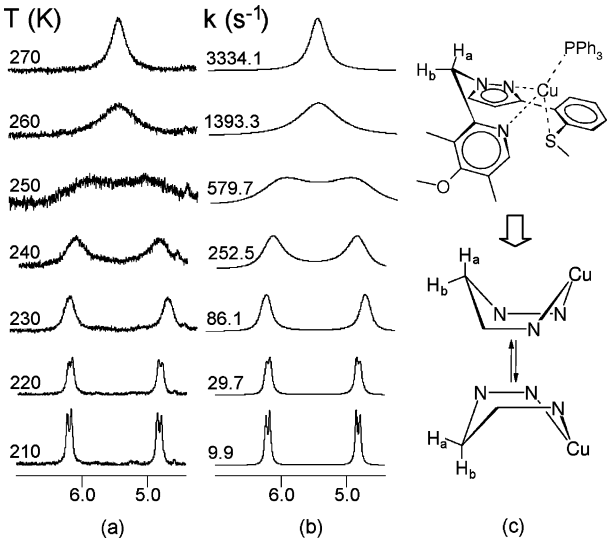

Figure 3. Experimental (a) and simulated (b) ^{1}H NMR spectrum of **2** in the region of the H_a and H_b diasterotopic protons. A description of the boat inversion process is reported in (c).

metal lies out of the trigonal plane by ~0.46 Å in the direction of S(11). The BF_4^- counterion is statically disordered in three positions that occupy a structural spherical site.

Complex **2** presents a fluxional behavior in solution, as shown by the ^{1}H VT NMR spectrum in $CDCl_3$, Figure 3. The bridging methylene of the ligand gives a broad signal at 270 K, which splits into two sharp doublets by lowering the temperature to 210 K, while the other peaks exhibit only a chemical shift temperature dependence. This behavior is justified with the diastereotopic nature of the methylene group at low temperatures, which can be explained in two ways: (a) the presence of the stereogenic Cu(I) center; (b) the boat conformation of the N,N′ chelate six-membered ring around the metal center. The kinetic parameters of the exchange process were determined from the complete line shape analysis[44,45] to be the following: $\Delta H^{\ddagger} = +43.6(3)$ kJ·mol^{-1}; $\Delta S^{\ddagger} = -16(1)$ J mol^{-1} K^{-1}. These values suggest a nondissociative rearrangement, which is most likely the inversion of the boat, as shown by some examples reported in the literature.[46−48] This implies a fast inversion (on the NMR time scale) around the Cu center, which probably involves the stretching or rupture of the labile Cu(I)−S-thioether bond.

Solid-State Structure, Solution Properties, and DFT Calculations for $[Cu_6(L)_2(C_6F_5S)_6]$ (3). By using the monodentate sulfur donor ligand $C_6F_5S^-$ as a coligand in place of PPh_3, additional complications became evident. The idea of obtaining a neutral copper(I) complex exhibiting an approximately tetrahedral structure with a N,N′,S,S′ donor set is difficult to fulfill, mainly because of the absence of steric hindrance on both **L** and on the thiolate group, which enables the thiolate to bridge metal centers. In the first stage, the 1:1:1 Cu:$C_6F_5S^-$:**L** stoichiometric ratio was employed for the synthesis, but this led nonetheless to the isolation and X-ray characterization of a 3:3:1 hexanuclear complex (**3a**). We therefore optimized the synthesis in 3:3:1 conditions to give **3**, which crystallized as **3a** by incorporating an acetonitrile molecule. An exemplified molecular drawing, depicting the coordination environment of the six copper atoms, is reported in Figure 4. The structure consists of six metal atoms, six thiolate groups, and two **L** ligands arranged in a clusterlike fashion. Cu(1) and Cu(2) are the only atoms that are bound to **L**, and they are located in the peripheral part of a $[Cu_4(C_6F_5S)_6]^{2-}$ copper−thiolate cluster. The four metals of the core adopt a trigonal geometry determined by bridging thiolate groups and, in the case of Cu(5), also by an acetonitrile molecule (crystallization solvent). The structure of the copper−thiolate cluster is likely derived from a closed $[Cu_4(C_6F_5S)_6]^{2-}$ adamantane-like structure,[15,17,49] by disruption of S−Cu−S links and subsequent insertion of CH_3CN, now bound to Cu(5) to give an "open" structure. The negative charge (2−) of the open $[Cu_4(C_6F_5S)_6CH_3CN]^{2-}$ cluster is compensated by two $[Cu(L)]^+$ peripheral moieties, which are bound to the former by means of thiolate groups. As a consequence of the open structure, three Cu−Cu interactions are shorter, ~2.8 Å (between Cu(4), Cu(5), and Cu(6)), and two are longer, ~3.4 Å (Cu(3)−Cu(4) and Cu(3)−Cu(6)). Interestingly, part of this structure reproduces that present in the core of the yeast copper metallothionein (Cu−MT),[20] a protein rich in cysteine residues that can bind up to eight copper(I) ions, six of which are in a trigonal

(44) Sandstrom, J. *Dynamic NMR Spectroscopy*; Academic Press: London, 1982.
(45) Reich, H. J. *WINDNMR software: NMR Spectrum Calculations*, version 7.1.11; 2005.
(46) Byers, P. K.; Canty, A. J.; Honeyman, R. T. *Adv. Organomet. Chem.* **1992**, *34*, 1−65.
(47) Tejel, C.; Villoro, J. M.; Ciriano, M. A.; Lopez, J. A.; Eguizabal, E.; Lahoz, F. J.; Bakhmutov, V. I.; Oro, L. A. *Organometallics* **1996**, *15*, 2967−2978.
(48) Antinolo, A.; Carrillo-Hermosilla, F.; Diez-Barra, E.; Fernandez-Baeza, J.; Fernandez-Lopez, M.; Lara-Sanchez, A.; Moreno, A.; Otero, A.; Rodriguez, A. M.; Tejeda, J. *J. Chem. Soc., Dalton Trans.* **1998**, 3737−3743.
(49) Janssen, M. D.; Grove, D. M.; vanKoten, G. *Prog. Inorg. Chem.* **1997**, *46*, 97−149.

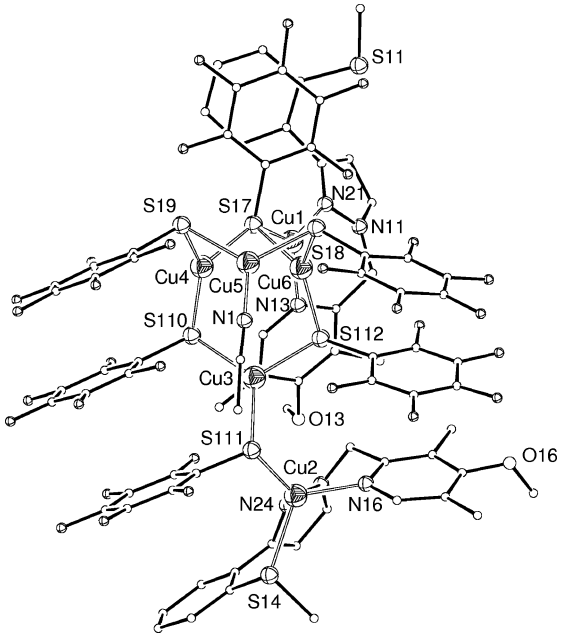

Figure 4. X-ray molecular structure of the copper(I)−SC_6F_5 cluster crystallized from an acetonitrile−water solution (**3a**). The hydrogen atoms have been omitted for clarity.

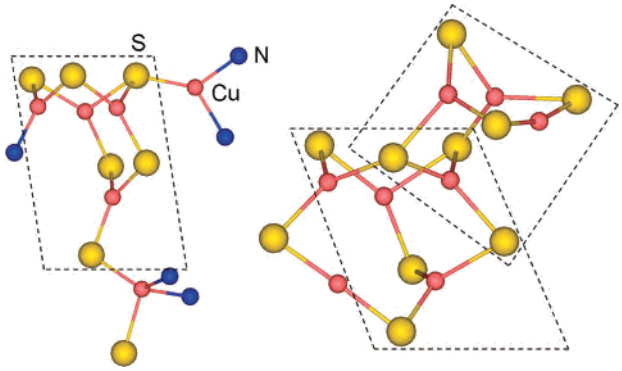

Figure 5. Copper−donor atom connectivity in **3a** (left) and in the yeast copper metallothionein (right). Structural analogies are highlighted in the dashed boxes.

geometry whereas two are in a digonal arrangement. It has been proposed that these two labile peripheral metals confer on the protein the ability to regulate copper homeostasis and they are also involved in the delivery of copper to apo-copper chaperones. Figure 5 reports, for comparison, the atom connectivity of the Cu−MT core and that found in **3a**. Even though the Cu−MT cluster is more complex and it hosts more metal ions, some similarities with **3a** are evident. It is interesting to note that the Cu−MT core may be imagined as a superposition of open $\{Cu_4S_6\}$ clusters.

When acetonitrile, which is present in the structure of **3a** (colorless crystals), is removed under vacuum, the deep yellow product **3** forms. This process is reversible: by addition of a few drops of acetonitrile, the product turns white. The complex **3** is luminescent in the solid state, emitting at 680 nm (excitation: 300 nm, 298 K, Figure 6), whereas in acetonitrile solution there is no evidence of emitting properties. This can be readily explained by a direct solvent−cluster interaction, also supported by the solid-state structure **3a**, that results in luminescence quenching. The

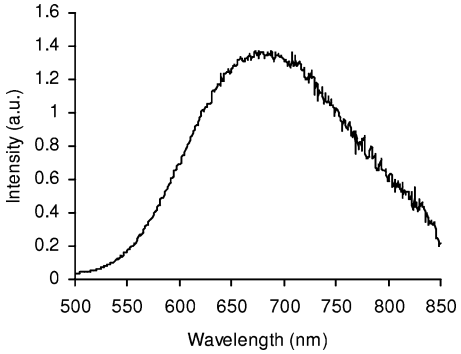

Figure 6. Emission spectrum of **3** (yellow powder) at 298 K, with an excitation wavelength of 300 nm.

large stoke shift (380 nm) is typical of multinuclear copper compounds.[50] On the basis of these observations and also according to known Cu(I) adamantane-like structures reported in the literature,[17,18] a closed adamantane-like structure (Scheme 3), derived from the X-ray structure by elimination of the coordinated acetonitrile and by the closure of S(111) on Cu(5), may be proposed for the yellow solid **3**.

Acetonitrile is the only common organic medium in which **3** is quite soluble, so that the solution characterization of **3** was performed in this solvent. The presence of a Cu(I)−thiolate cluster in solution is confirmed by the ESI-mass spectrometry and by ^{19}F PGSE NMR experiments. In particular, the mass spectrum in negative ionization mode reveals the presence of monoanionic $[Cu_n(C_6F_5S)_{n+1}]^-$ (n = 1−5) fragments of the cluster (Supporting Information, Figures S4 and S5), whereas in positive ionization mode, only the $[Cu(L)]^+$ fragment is present. This could arise during the ESI-mass ionization process or be present in solution according to a ionic dissociation equilibrium: **3a** + CH_3CN = $[Cu_4(C_6F_5S)_6]^{2-}$ (**3b**) + $2[Cu(L)CH_3CN]^+$ (see Scheme 3). The latter hypothesis is in agreement with conductivity measurements performed on a 10^{-3} M solution of **3**, which afford a molar conductivity value of 131(1) Ω^{-1} cm^2 mol^{-1}, slightly less than the range reported for 1:2 electrolytes in acetonitrile (145−336 Ω^{-1} cm^2 mol^{-1}).[51] This would give credit to the hypothesis of the ionic dissociation of **3a** in solution.

^1H and ^{19}F PGSE NMR experiments were performed to obtain the hydrodynamic radius (r_H) and volume (V_H) of **3**. The measurements based on ^{19}F afford a r_H of 6.8(1) Å and a V_H of 1300(60) $Å^3$, while the ^1H PGSE values point to significantly smaller dimensions (r_H = 5.2(1) Å and V_H = 600(30) $Å^3$). This discrepancy can be explained by considering the aforementioned dissociation equilibrium: the ^{19}F nucleus, in fact, is present only in the exhanging **3a**,**b** clusters (large), while protons are shared by **3a** (large) and $[Cu(L)CH_3CN]^+$ (small). Hence, the V_H value derived from ^1H PGSE ($V_H(^1H)$) would correspond to the weighted average between the volumes of **3a** and $[Cu(L)CH_3CN]^+$ and should result as significantly smaller than $V_H(^{19}F)$. In addition, a comparison between the experimental $V_H(^1H)$ with the van

(50) Ford, P. C.; Cariati, E.; Bourassa, J. *Chem. Rev.* **1999**, *99*, 3625−3647.
(51) Geary, W. J. *Coord. Chem. Rev.* **1971**, *7*, 81−122.

Scheme 3

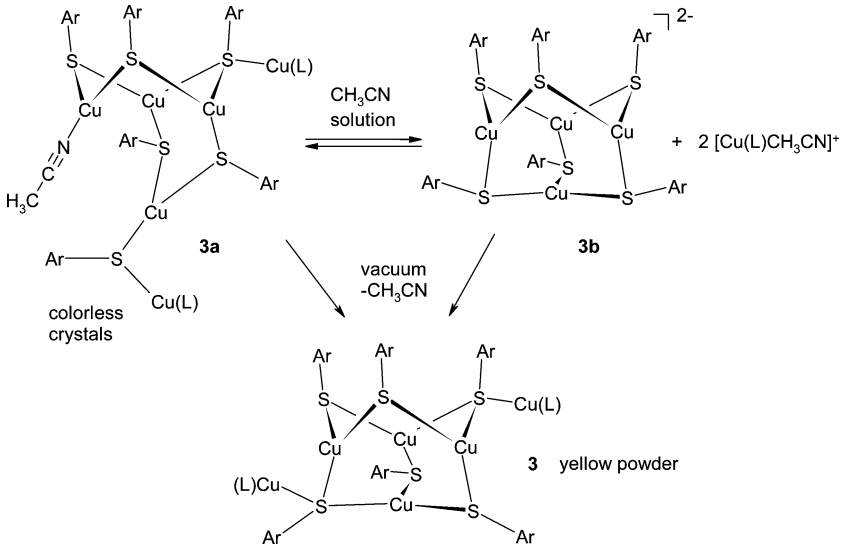

Table 3. Computed Energetic Properties in the Gas Phases, E (0 K) and G_{298} (298 K), and in Solution, G^{solv}, for the Mononuclear and Polynuclear Structures Reported in Figure 7 (B3LYP/lanl2dz) ($\Delta G^{solv} = G^{solv} - E$)[a]

compd	E (hartree)	G_{298} (hartree)	G^{solv} (hartree)	ΔG^{electr} (kJ mol^{-1})	$\Delta G^{nonelectr}$ (kJ mol^{-1})	ΔG^{solv} (kJ mol^{-1})
[Cu(L′)(C_6H_5S)]	−1230.876 04	−1230.564 33				
[Cu_6(L′)$_2$(C_6H_5S)$_6$]	−4213.597 08	−4212.626 77	−4213.548 92	−228.4	354.9	126.5
L′	−792.926 75	−792.695 38				
[Cu(L′)CH_3CN]$^+$	−1121.721 64	−1121.449 57	−1121.753 96	−176.5	91.7	−84.8
[Cu_4(C_6H_5S)$_6$]$^{2-}$	−2235.355 89	−2234.899 41	−2235.523 92	−613.9	172.7	−441.2
CH_3CN	−132.728 28	−132.706 77	−132.728 42	−23.2	22.8	−0.4
[Cu_4(C_6H_5S)$_6$$CH_3CN$]$^{2-}$	−2368.099 57	−2367.605 32	−2368.257 63	−614.7	199.7	−415.0

[a] $\Delta G^{nonelectr} = \Delta G^{cav} + \Delta G^{rep} + \Delta G^{disp}$; 1 hartree = 2625.5 kJ mol^{-1}

der Waals volumes (V_{VdW}) of **3a** (1228 Å^3) and [Cu(L)CH_3-CN]$^+$ (327 Å^3) would suggest only a partial ionic dissociation of **3a**, since V_H(^{1}H) is intermediate between the above-mentioned values. On the other hand, by considering the solvent-excluded volume (V_{soft}) as an estimate of the hydrodynamic volume of the respective species (2039 Å^3 for **3a** and 605 Å^3 for [Cu(L)CH_3CN]$^+$), we infer a nearly complete ionic dissociation, as V_H(^{1}H) becomes comparable to the V_{soft} of [Cu(L)CH_3CN]$^+$. Since V_{VdW} represents the lower limit of V_H[52] and assuming that V_{soft} represents the upper V_H limit, the dissociation of **3a** is partial or complete according to which theoretical volume, V_{VdW} or V_{soft}, is taken as reference. However, a complete ionic dissociation appears quite plausible, as attested by the following evidence: (1) As stated above, the molar conductivity is close to that reported for completely dissociated 1:2 electrolytes in acetonitrile. (2) No peaks of a [Cu_n(L)(C_6F_5S)$_{n+1}$]$^-$ species appear in the ESI-mass spectrum. (3) Both the ^{1}H and ^{19}F NMR spectra exhibit only a set of signals, and it would be consistent with the presence of a more symmetrical **3b** species (if compared to **3a**) and [Cu(L)CH_3CN]$^+$. If this is not the case, a fast-exchange equilibrium with **3a** should be invoked.

To further support the hypothesis that a Cu(I)−thiolate cluster structure is energetically favored over a mononuclear complex, DFT calculations were performed to compute the free energy of the gas-phase reaction 6[Cu(L′)(C_6H_5S)] → [Cu_6(L′)$_2$(C_6H_5S)$_6$] + 4L′ as well as to evaluate the stability of the hexanuclear cluster in acetonitrile solution (Tables 3 and 4 and Figure 7). The $C_6H_5S^-$ thiolate was employed instead of the less electron-donating $C_6F_5S^-$ to save computational resources, so some caution is required when inferring properties of the real system by using these models. As an example, the comparison between the [Cu(L′)(C_6H_5S)] and [Cu(L′)(C_6F_5S)] optimized models reveals that in the former case the copper geometry is trigonal planar with the thioether sulfur not coordinated, whereas in the latter the metal geometry is tetrahedral with the thioether bound to copper and a longer Cu−SC_6F_5 bond distance (Figure S2 of the Supporting Information). This comes as a consequence of the minor donor ability of the fluorinated thiolate as evidenced from a comparison of the natural bond orbital

Table 4. Computed Thermodynamic Properties for Gas- (ΔE, ΔE_{298}, ΔG_{298})[a] and Solution-Phase ($\Delta G^{solution}$)[b] Reactions a−c Reported in Figure 7 (kJ mol^{-1}, B3LYP/lanl2dz)

reacn	ΔE	ΔE_{298}	ΔG_{298}	$\Delta G^{solution}$
a	−125.6	−114.0	−58.6	
b	668.1	682.5	634.7	−101.8
c	−40.4	−23.5	2.3	28.8

[a] Calculated as the difference between the corresponding thermodynamic properties of products and reactants, $\Delta G_{298} = \Sigma G_{Product} - \Sigma G_{Reactant}$. [b] Calculated according to the thermodynamic cycle reported in Scheme 2, $\Delta G^{solution} = \Delta G_{298} + \Delta\Delta G^{solv}$.

(52) Zuccaccia, D.; Bellachioma, G.; Cardaci, G.; Ciancaleoni, G.; Zuccaccia, C.; Clot, E.; Macchioni, A. *Organometallics* **2007**, *26*, 3930−3946.

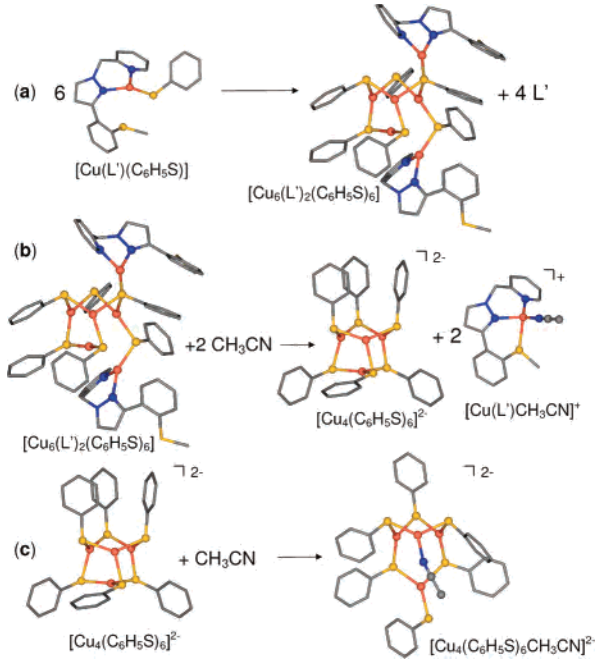

Figure 7. Optimized molecular structures for the Cu(I)/L′/$C_6H_5S^-$ system (B3LYP/lanl2dz): (a) oligomerization reaction 6[Cu(L′)(C_6H_5S)] → [Cu_6(L′)$_2$(C_6H_5S)$_6$] + 4L′; (b) ionic dissociation of the [Cu_6(L′)$_2$(C_6H_5S)$_6$] cluster; (c) acetonitrile interaction with the $[Cu_4(C_6H_5S)_6]^{2-}$ cluster.

charges[53] of the sulfur atom calculated for $C_6H_5S^-$ and $C_6F_5S^-$ (Figure S3 of the Supporting Information). These considerations should be kept in mind during the following discussion, where the thermodynamic properties are illustrated for the optimized molecular structures reported in Figure 7. The in vacuo free energy of reaction (ΔG_{298}) for the production of the cluster from mononuclear entities is −58.6 kJ mol^{-1}, supporting the stability of the former. This is in agreement with previous DFT calculations performed on cyclic copper(I)−thiolate assemblies showing that oligomerization is energetically favored.[54] The $[Cu_4(C_6H_5S)_6]^{2-}$ inner core of the [Cu_6(L′)$_2$(C_6H_5S)$_6$] optimized structure presents three copper atoms in trigonal planar arrangements and one copper atom in a distorted digonal geometry. The two outer trigonal copper centers are bound by two κ^2-N,N′ ligands, and they are linked to the $[Cu_4(C_6H_5S)_6]^{2-}$ unit by bridging thiolates. We propose that this structure may model that adopted by **3** when acetonitrile is removed under vacuum (see Scheme 3).

Since there is experimental evidence that the two peripheral $[Cu(L)]^+$ moieties of **3** may be subject to dissociation from the $[Cu_4(C_6H_5S)_6]^{2-}$ cluster in acetonitrile solution, we computed the energetics of this reaction to substantiate this hypothesis (Figure 7b). The computed ΔE and ΔG_{298} of the ionic dissociation reaction are positive in the gas phase (668.1 and 634.7 kJ mol^{-1}, respectively), pointing to a considerable stabilization of the neutral [Cu_6(L′)$_2$(C_6H_5S)$_6$] assembly. However, if we take into account the effect of the solvent and, in particular, the stabilization that derives from a polar solvent such as acetonitrile on the ionic products of the reaction, it appears that the reaction is exergonic ($\Delta G^{solution}$ = −101.8 kJ mol^{-1}), making the dissociation even more favored in the presence of a large excess of solvent.

The reaction reported in Figure 7c describes the "opening" of the closed $[Cu_4(C_6H_5S)_6]^{2-}$ cluster by acetonitrile. The gas-phase reaction is exothermic (ΔE = −40.4 kJ mol^{-1}) but endergonic (ΔG_{298} = +2.3 kJ mol^{-1}) since it is entropically disfavored. Moreover, the reaction is even more endergonic in CH_3CN solution ($\Delta G^{solution}$ = +28.8 kJ mol^{-1}), suggesting the greater stability of the closed $[Cu_4(C_6H_5S)_6]^{2-}$ cluster with respect to the open form. This is in agreement with the proposed **3b** structure, which is supported also by the absence of CH_3CN in all of the ESI-mass fragments and by the reported crystallization of $[(C_6H_5)_4P]_2[Cu_4(SC_6H_5)_6]$ from acetonitrile, in which the cluster is in the closed form.[18]

Conclusions

The coordination capabilities of the N,N′,S ligand 4-methoxy-3,5-dimethyl-2-((3-(2-(methylthio)phenyl)-1*H*-pyrazol-1-yl)methyl)pyridine (**L**) were evaluated with Cu(I). Since the ligand possesses a weakly coordinating thioether group, ancillary monodentate ligands were employed (PPh_3 and $C_6F_5S^-$) to complete the copper coordination requirements. However, as evidenced by the X-ray structures, the nuclearity of the complexes cannot be easily controlled, and only the ternary complex $[Cu(L)PPh_3]BF_4$ (**1**) is mononuclear, whereas the **L**/Cu(I) binary mixture in acetonitrile produces two cocrystallized entities: a monomeric $[Cu(L)CH_3CN]^+$ and a dinuclear $[Cu_2(L)_2CH_3CN]^{2+}$complex. In addition, the ternary Cu(I)/**L**/$C_6F_5S^-$ system gives rise to the isolation of a polynuclear compound, [Cu_6(L)$_2$(C_6F_5S)$_6CH_3CN$] (**3a**), which bears similarities to an open adamantane-like {Cu_4S_6} cluster. Part of this copper(I)−thiolate framework is found in the structure of the yeast metallothionein core, which exhibits eight copper(I) metals bound by cysteinate residues. The propensity of the thiolate ligands to bridge metal centers is probably the driving force that leads to the isolation of a multinuclear structure. This is also evidenced by DFT calculations that show how the hexanuclear unit is favored, in the gas phase, over a hypothetical mononuclear complex. So, to better control the nuclearity of Cu(I) centers, especially in presence of thiolates, it would be necessary to employ a more sterically demanding and preorganized ligand.[55] This can be obtained, for example, by functionalization of the prochiral methylene group of **L** with proper donor moieties to yield tetradentate N,N′,S,S′ heteroscorpionates, which may alone satisfy the electronic and steric requirement of copper(I) without additional monodentate coligands.

Acknowledgment. This work was supported by the Ministero dell'Istruzione, dell'Università e Ricerca (Rome, Italy).

Supporting Information Available: CIF files for **L**, **1**, **2**, and **3a**, an Ortep molecular structure of **L**, DFT-optimized geometries

(53) Reed, A. E.; Curtiss, L. A.; Weinhold, F. *Chem. Rev.* **1988**, *88*, 899−926.
(54) Howell, J. A. S. *Polyhedron* **2006**, *25*, 2993−3005.
(55) Fujisawa, K.; Fujita, K.; Takahashi, T.; Kitajima, N.; Moro-oka, Y.; Matsunaga, Y.; Miyashita, Y.; Okamoto, K. *Inorg. Chem. Commun.* **2004**, *7*, 1188−1190.

(B3LYP/lanl2dz) of the mononuclear models [Cu(L′)(C_6H_5S)] and [Cu(L′)(C_6F_5S)], NBO charges of $C_6H_5S^-$ and $C_6F_5S^-$, Cartesian coordinates of the optimized structures **L′**, [Cu(**L′**)CH_3CN]$^+$, [Cu(**L′**)(C_6H_5S)], [$Cu_4(C_6H_5S)_6$]$^{2-}$, [$Cu_4(C_6H_5S)_6CH_3CN$]$^{2-}$, and [Cu_6(L′)$_2(C_6H_5S)_6$], ^{1}H and ^{19}F PGSE NMR experimental details for **3**, and the ESI-mass spectrum and isotopic pattern of **3**. This material is available free of charge via the Internet at http://www.pubs.acs.org.

IC701189B